Eur. Phys. J. B **4**, 159–167 (1998)

THE EUROPEAN PHYSICAL JOURNAL B

Charge states of transition metal in "Cr, Co and Ni" doped $Ln_{0.5}Ca_{0.5}MnO_3$ CMR manganites

O. Toulemonde, F. Studer[a], A. Barnabé, A. Maignan, C. Martin, and B. Raveau

Laboratoire CRISMAT[b], associée au CNRS, ISMRA, boulevard Maréchal Juin, 14050 Caen Cedex, France

Received: 9 January 1998 / Received in final form: 6 April 1998 / Accepted: 7 April 1998

Abstract. The XAS study at Cr, Co, Ni and Mn K-edges was performed for the doped CMR manganites $Ln_{0.5}Ca_{0.5}Mn_{1-x}B_xO_3$ with Ln=La, Nd, Sm and B= Cr, Co, Ni ($0 \leq x \leq 0.10$), on the samples that were studied previously for their ferromagnetic-metallic to antiferromagnetic-insulator transition. We observed that the formal charges of the doping elements are Ni^{2+}, Co^{2+} and Cr^{3+}. It is also evidenced that the average formal charge of the manganese is increased after doping, in agreement with the charge compensation keeping "O_3" stoichiometry. These results suggest that the doping elements participate directly to the band structure.

PACS. 78.70.Dm X-ray absorption spectra – 75.70.Pa Giant magnetoresistances – 71.30.+h Metal-insulator transitions and other electronic transitions

1 Introduction

Extensive studies of the manganese oxide perovskites $Ln_{1-x}A_xMnO_3$ (Ln = Re; A = Ca, Sr or Ba) have been carried out especially in the past from years after the discovery of giant or even colossal magneto-resistance (CMR) in these compounds [1–8].

Such colossal negative magneto-resistance properties originate from a double exchange (DE) mechanism between Mn(III) and Mn(IV) species [9–11] which has been proposed to create the ferromagnetism in competition with the superexchange mechanism inducing antiferromagnetic ordering. Like the HTC superconductors, the manganese oxides are highly correlated systems in which the metallic properties are created by hole doping: as a consequence a metallic conductivity can be induced at low temperature which could be due to doping holes in a $2p$ oxygen band. The antiferromagnetic coupling of these holes to the Mn^{3+} would be at the origin of the ferromagnetic ordering that appears in theses oxides.

Besides the DE mechanism, a polaronic type model based on the Jahn-Teller distortion of the MnO_6 octahedra has recently been proposed [12]. Neutron diffraction studies of these manganites showing structural evolution [13,14], and XAS studies at the Mn L_3-edge [15] showing changes in the local distorsion of the MnO_6 octahedra support this model. Nevertheless, EXAFS studies at manganese K-edge [16–18], which show an unusual change of the Debye-Weller parameter σ^2 at the insulator to metal transition, may be interpreted as either a dynamic Jahn-Teller distortion or a breathing mode of the octahedra. Up to now, it is impossible to distinguish between this two distorsion modes.

Among the different manganites, the oxides $Ln_{0.5}Ca_{0.5}MnO_3$, exhibit a particular behaviour due to the existence of charge ordering (CO) phenomena. It is for instance the case of the manganite $Pr_{0.5}Ca_{0.5}MnO_3$, for which a semi-conducting behaviour down to 4.2 K is observed. For this phase, contrary to many other manganites, no metal to insulator transition is observed. Moreover the magnetic ordering in these oxides is limited to a weak ferromagnetic coupling down to 150 K, followed by an antiferromagnetic ordering at lower temperatures.

Recently, an insulator-metal transition could be induced in $Ln_{0.5}Ca_{0.5}MnO_3$ by doping the Mn sites with transition metal elements such as cobalt, nickel or chromium [19–21]. For these Mn site doped manganites, the $R(T)$ curves exhibit a peak at temperature T_m, characteristic of the insulator-metal transition, whereas the magnetization curves $M(T)$, show a transition from an antiferromagnetic to a ferromagnetic state, with $T_c = T_m$, as illustrated for the manganites $Nd_{0.5}Ca_{0.5}(Mn_{1-x}Co_x)O_3$ (Fig. 1) and $Sm_{0.5}Ca_{0.5}(Mn_{1-x}Cr_x)O_3$ (Fig. 2) with x ranging for 0.02 to 0.10 [21].

From such experiments, we have to understand how such a small doping is able to induce so spectacular changes of the transport and magnetic properties of manganites. This suggests either that the doping cations participate strongly and directly to the changes in the electronic structure or that the doping cations induce indirectly changes in magnetic and transport properties of the manganese network. In both cases the knowledge of the valence states of the doping elements which reflect

[a] e-mail: studer@crindy.ismra.fr
[b] UMR 6508

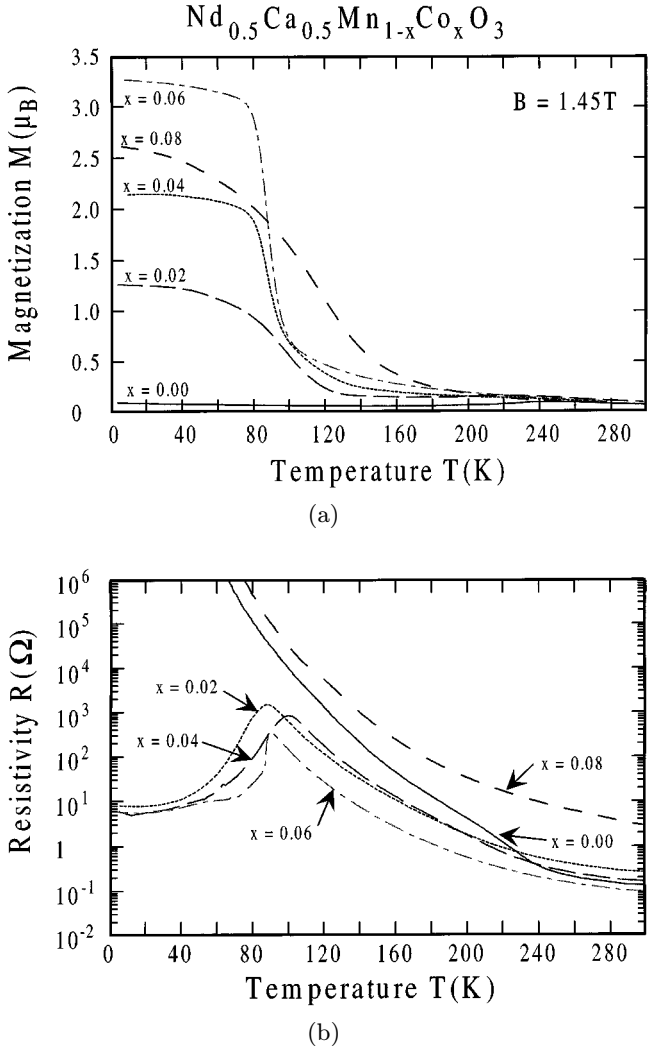

Fig. 1. (a) Magnetization *versus* temperature for the series of manganites $Nd_{0.5}Ca_{0.5}(Mn_{1-x}Co_x)O_3$. (b) Resistivity *versus* temperature for the series of manganites $Nd_{0.5}Ca_{0.5}(Mn_{1-x}Co_x)O_3$.

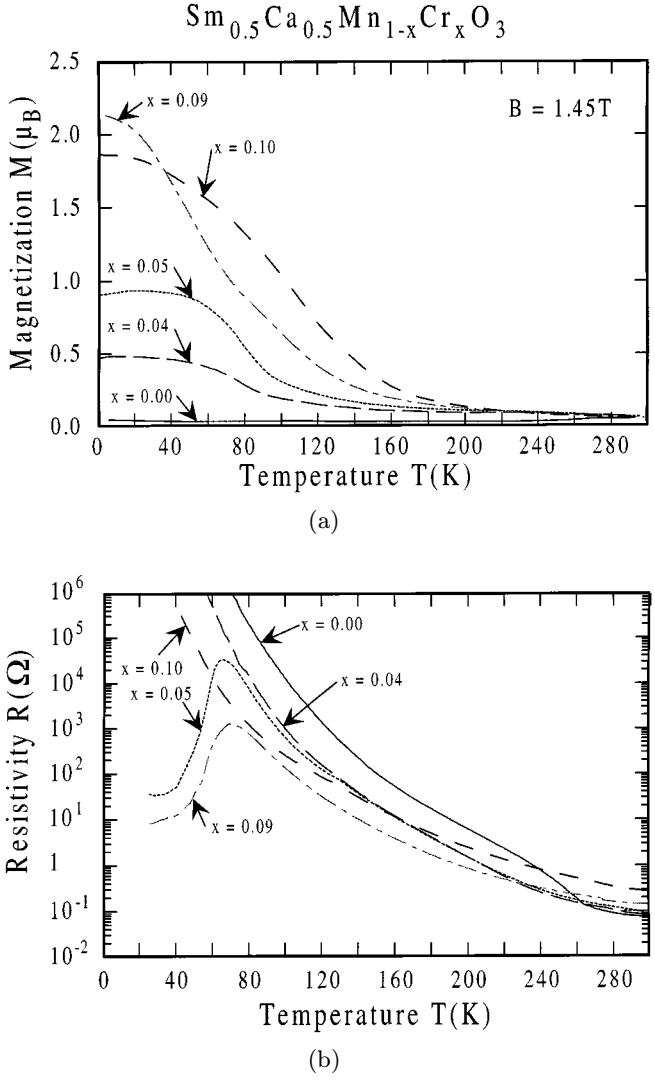

Fig. 2. (a) Magnetization *versus* temperature for the series of manganites $Sm_{0.5}Ca_{0.5}(Mn_{1-x}Cr_x)O_3$. (b) Resistivity *versus* temperature for the series of manganites $Sm_{0.5}Ca_{0.5}(Mn_{1-x}Cr_x)O_3$.

their electronic structure is of importance for the understanding of the changes in the physical properties of the $Ln_{0.5}Ca_{0.5}MnO_3$ manganites before and after doping.

X-ray Absorption Spectroscopy has been proven to be a valuable technique to investigate the valence states of elements in a complex material [22–25]. Specially recent studies of the CMR manganites at the manganese K-edge have shown that the average oxidation state of manganese is in good agreement with the stoichiometric one deduced from the substitution rate [26–28].

In this paper we present an XAS study at Cr, Co and Ni K-edges in doped $Ln_{0.5}Ca_{0.5}(Mn_{1-x}B_x)O_3$ (Ln = La, Pr, Nd, Sm; B = Cr, Co, Ni; $0.05 \leq x \leq 0.10$) compounds in order to determine the valence states of these elements. A similar XAS study at Mn K-edge is also presented in correlation with magnetic and electron transport properties.

2 Experimental

The doped manganites $Ln_{0.5}Ca_{0.5}(Mn_{1-x}B_x)O_3$ were prepared in the form of sintered pellets following a classical method of solid state chemistry. Thorough mixtures of oxides CaO, Mn_2O_3, Cr_2O_3 or Co_3O_4 or NiO, La_2O_3 or Nd_2O_3 or Pr_6O_{11} or Sm_2O_3 were first heated in air at 950 °C for 12 hours. The samples were then pressed into pellets and sintered first at 1200 °C and then at 1500 °C for 12 hours in air.

Magnetization curves $M(T)$ were established with a vibrating sample magnetometer. Sample were first zero field cooled and then the magnetic field was applied at 5 K. Measurements were carried out under warming. Resistance measurements were performed with the four probe technique on sintered bars with $2\times2\times10$ mm^3 dimensions. Magneto-resistance measurements were performed with a

Quantum Design physicals properties measurements systems (PPMS). Resistance was measured with decreasing temperature in magnetic fields of 0 and 7 T.

The X-ray absorption study of these phases was performed systematically on the samples previously studied for their transport and magnetic properties.

The X-ray absorption spectra at Cr, Mn, Co and Ni K-edges were recorded at room temperature in a classical transmission mode at the EXAFS I station (channel cut monochromator) using the synchrotron radiation of the DCI storage ring of LURE (Orsay, France) working at 1.85 GeV with a 250 mA current. The energy resolution at Co K-edge is estimated to 1.3 eV whereas the reproducibility of the monochromator position is as high as 0.3 eV.

The normalization procedure used throughout this work was a standard one: after substraction of the same diffusion background on the XANES and EXAFS spectra, recorded in the same experimental conditions, a point located at an energy of 800 eV from the edge, where no more EXAFS oscillations were still observable, was set to unity. Then the intensity of a point with an energy between 50 and 100 eV from the edge was recorded on the EXAFS spectrum and reported on the XANES to set the normalized height.

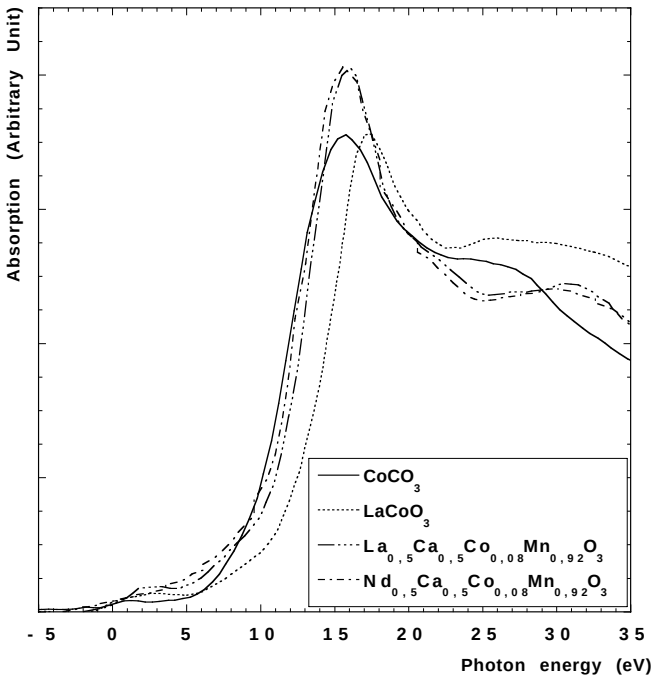

Fig. 3. Normalized Co K-edges at room temperature for some cobalt oxide references and $Ln_{0.5}Ca_{0.5}Mn_{0.92}Co_{0.08}O_3$ (Ln=La; Nd).

3 Results and discussion

3.1 Cobalt K-edge

The cobalt K-edges of some reference compounds, $CoCO_3$ and $LaCoO_3$ for Co^{2+} and Co^{3+} respectively, in a regular octahedral environment, and of two substituted manganites, $La_{0.5}Ca_{0.5}(Mn_{0.92}Co_{0.08})O_3$ and $Nd_{0.5}Ca_{0.5}(Mn_{0.92}Co_{0.08})O_3$, are shown in Figure 3. The energy gap between the $CoCO_3$ and $LaCoO_3$ edges ($\approx$ 1.5 eV) is 5 times higher than the reproducibility of the monochromator position. Both the energies of the midheight of the main absorption jump and the calculated mean edge energies for the four compounds (Tab. 1) [29–32] allow to conclude that cobalt is in the Co^{2+} formal state in the substituted manganites within the experimental error on such a determination estimated to $\pm$ 10%. Note that the long Co-O distances in $CoCO_3$ (Tab. 1) can explain for the strong shift of the edge of this compound towards low energy as compared to $LaCoO_3$ in the framework of the so-called Natoli's rule [33] which can be written as $(E - E_0)R^2 = K$ where E and R are the peak energy and M-O distance respectively, E_0 and K being constants. This result is in agreement with a former XAS observation [34] at cobalt L_3-edge of some other manganites with composition $La_{0.7}Sr_{0.3}(Mn_{0.8}Co_{0.2})O_3$ and $La(Mn_{0.85}Co_{0.15})O_3$ which concluded also to the presence of Co^{2+} formal charge.

3.2 Nickel K-edge

The results are also very conclusive for the nickel substitution as shown in Table 1 and Figure 4 for manganites

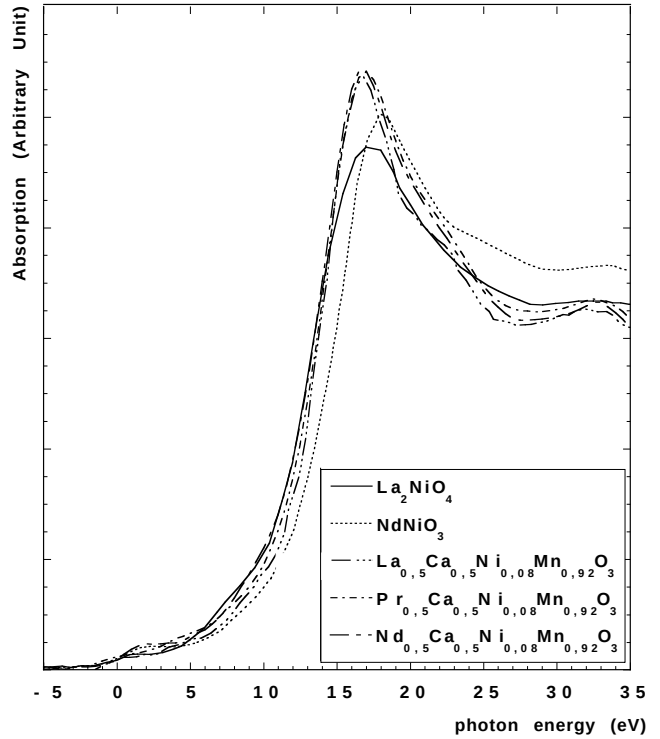

Fig. 4. Normalized Ni K-edges at room temperature for some nickel oxide references and $Ln_{0.5}Ca_{0.5}Mn_{0.92}Ni_{0.08}O_3$ (Ln=La; Nd; Pr).Normalized Ni K-edges at room temperature for some nickel oxide references and $Ln_{0.5}Ca_{0.5}Mn_{0.92}Ni_{0.08}O_3$ (Ln=La; Nd; Pr).

Table 1. Formal charge, $d_{\mathrm{M-O}}$ (M=Co and Ni), energy of main jump midheight and equivalent energies from edge integration at Co and Ni K-edge for references and doped manganites compounds.

compounds	formal charge Co	$d_{\mathrm{Co-O}}$ in angström	energy of main jump midheight (eV) ± 0.3 eV	equivalent energies from edge integration (eV) ± 0.3 eV	references
$CoCO_3$	+2	Co(1):6 × 2.11	11.5	8.0	[29]
$LaCoO_3$	+3	Co(1):6 × 1.92	14.2	11.2	[30]
$La_{0.5}Ca_{0.5}Co_{0.08}Mn_{0.92}O_3$	+2		12.6	8.3	
$Nd_{0.5}Ca_{0.5}Co_{0.08}Mn_{0.92}O_3$	+2		12.0	7.6	
compounds	formal charge Ni	dNi–O in angström	energy of main jump midheight (eV) ± 0.3 eV	equivalent energies from edge integration (eV) ± 0.3 eV	
La_2NiO_4	+2	Ni(1):4 × 1.94 2 × 2.28	12.7	9.1	[31]
$NdNiO_3$	+3	Ni(1):2 × 1.935 2 × 1.945, 2 × 1.950	14.2	10.7	[32]
$La_{0.5}Ca_{0.5}Ni_{0.08}Mn_{0.92}O_3$	+2		13.5	9.3	
$Nd_{0.5}Ca_{0.5}Ni_{0.08}Mn_{0.92}O_3$	+2		13.0	8.5	
$Pr_{0.5}Ca_{0.5}Ni_{0.08}Mn_{0.92}O_3$	+2		13.3	8.9	

with composition $Ln_{0.5}Ca_{0.5}(Mn_{0.92}Ni_{0.08})O_3$ (Ln = La, Pr, Nd). The nickel K-edges of the three nickel substituted compounds exhibit edge energies close to the one of La_2NiO_4, reference oxide for Ni^{2+} formal state. Here again the energy gap (≈ 1.5 eV) between La_2NiO_4 and $NdNiO_3$ synthesized by Lacorre at the Université du Maine (Le Mans, France), reference for Ni^{3+} formal state, is much higher than the reproducibility of the monochromator position. Note also that the spread of Ni-O distances in two sets for La_2NiO_4 can account for the shape and width of the edge. Like for the cobalt substitution, nickel appears to be in the Ni^{2+} formal state in the nickel doped manganites.

3.3 Chromium K-edge

The chromium K-edges of four reference oxides, Cr_2O_3 [35] and $NdCrO_3$ [36] for Cr^{3+}, CrO_2 [37] for Cr^{4+} and $K_2Cr_2O_7$ [38] for Cr^{6+}, are shown in Figure 5a. The difference between Cr_2O_3 and $NdCrO_3$ arises from the distortion of the oxygen octahedron around chromium cation. The regular octahedron in $NdCrO_3$ with 6 comparable Mn-O distances ($d_{\mathrm{Mn-O}} \approx 1.98$ Å) generates a strong white line at 17.6 eV due to the combined electronic transitions $1s \rightarrow 4p_{x,y,z}$. Conversely the octahedral distortion in Cr_2O_3 with two sets of Mn-O distances ($3d_{\mathrm{Mn-O}} \approx 1.95$ Å; $3d_{\mathrm{Mn-O}} \approx 2.04$ Å) induces a wide spread of the $1s \rightarrow 4p$ transitions along the x, y and z-axis respectively. In both cases a small prepeak is observed with a fine structure of two peaks (1.8 and 5 eV) for Cr_2O_3 and three peaks for $NdCrO_3$ (2, 5.5 and 7.6 eV). This prepeak is often observed in transition metal compounds and is due to an hybridization of Cr($3d$)-O($2p$)-Cr($4p$) orbitals. This hybridization is stronger in noncentrosymmetric environment and allows partly the forbidden $1s \rightarrow 3d$ transition to be visible. For both studied Cr^{3+} oxides, the small intensity of the prepeak is in agreement with an octahedral, although distorted, environment of chromium. The fine structure observed in both oxides (A_1, A_2 for Cr_2O_3; A'_1, A'_2 and A'_3 for $NdCrO_3$) is due to the crystal field effect on the Cr $3d$ orbitals (t_{2g} and e_g) plus the splitting between spin up and spin down electronic levels due to the Coulombian repulsion U. Taking into account the Cr^{3+} electronic state ($3d^3$) which fills up only the $t_{2g}^{\uparrow}$ lowest levels leaving three empty molecular orbitals $t_{2g}^{\downarrow}$, $e_g^{\uparrow}$ et $e_g^{\downarrow}$. The observation of these empty levels depends on the relative interplay of the experimental energy resolution and on the splitting induced by the crystal field strength 10 Dq, on $3d$ and $4p$ orbitals, and the Hubbard's repulsion parameter U.

The K-edge of CrO_2 was obtained from a thin film synthesized by Barry at the Trinity College (Dublin). It is ferromagnetic and exhibits a metallic conductivity. The CrO_2 spectrum of Figure 5a, with a small prepeak and

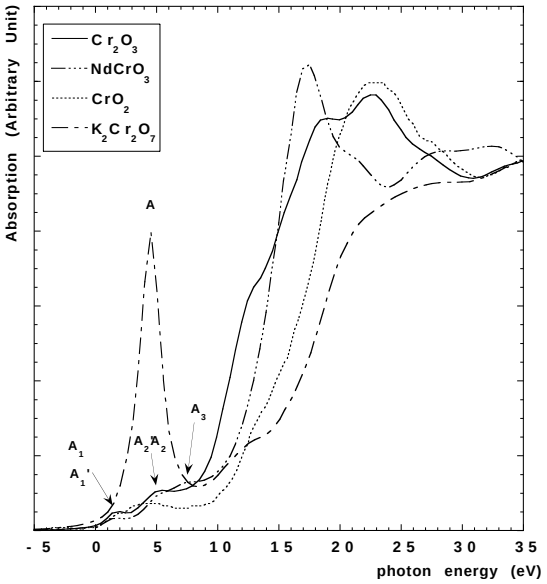

(a)

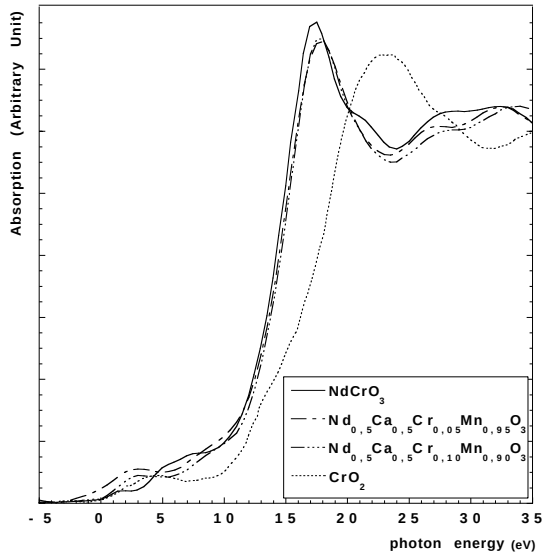

(b)

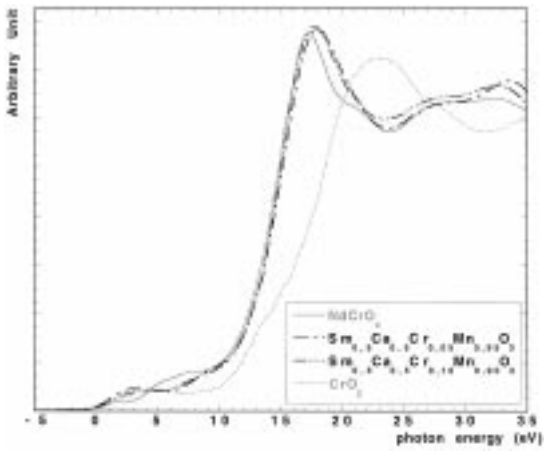

(c)

Fig. 5. (a) Normalized Cr K-edges at room temperature for chromium references. (b) Normalized Cr K-edges at room temperature for chromium references and $Nd_{0.5}Ca_{0.5}Mn_{1-x}Cr_xO_3$ ($x = 0.05$ and 0.10). (c) Normalized Cr K-edges at room temperature for chromium references and $Sm_{0.5}Ca_{0.5}Mn_{1-x}Cr_xO_3$ ($x = 0.05$ and 0.10).

a single main line at 22 eV, is clearly characteristic of a regular octahedral environment around Cr^{4+} ions. It is worth noting that, for the same overall composition, only the Cr_2O_3 spectrum was previously observed [39] from soft X-ray absorption due to the fact that the latter technique is more surface sensitive. In contrast our experiment is bulk sensitive due to the depth probed by the high energy photon at the K-edge.

In the case of $K_2Cr_2O_7$, reference oxide for the Cr^{6+} formal charge, a very intense prepeak is observed (Fig. 5a) in agreement with the tetrahedral oxygen environment and the high density of holes in the $3d$ shell. The width of the edge itself and the smooth XANES features above 20 eV are consistent with the spread of Cr-O distances (1.51 Å $< d_{Cr-O} <$ 1.86 Å) distributed over four different chromium sites. The energies of the main aborption jump and the equivalent ones are reported in Table 2 and are different from the octahedral chromium compounds.

The Cr K-edges of four chromium doped manganites $Ln_{0.5}Ca_{0.5}(Mn_{1-x}Cr_x)O_3$ (Ln=Nd; Sm; $x = 0.05$ and 0.1) are shown in Figures 5b and 5c together with two of the reference oxides $NdCrO_3$ and CrO_2. The edge energies of the doped compounds (Tab. 2) [35–38] correspond to a Cr^{3+} formal charge different from the formal charges of cobalt and nickel in manganites with the same composition. Such a result is interesting when considering the external electronic structure of purely ionic Cr^{3+} which is a $3d^3$ cation like Mn^{4+}. This suggest a substitution of either Mn^{3+} or Mn^{4+} subnetworks by Cr^{3+} cations. This will be discussed later on after the Mn K-edge study. The Cr K-edges of chromium doped lanthanum manganites could not be recorded in good conditions owing to the presence of the EXAFS oscillations of the La L_2-edge close to the Mn K-edge.

3.4 Manganese K-edges

The manganese K-edges of four reference compounds, Mn_2O_3 and $LaMnO_3$ for Mn^{3+} formal charge and MnO_2 and $CaMnO_3$ for Mn^{4+} formal charge in octahedral symmetry, are shown in Figure 6a. The consideration of the edge positions at midheight of the main absorption jump or of the calculated equivalent energies (Tab. 3) [40–43], shows that the reference spectra consist of two subsets separated by 3.2 eV with a small dispersion, corresponding to Mn^{3+} and Mn^{4+} respectively. The changes in shape arise from the distortion of the oxygen octahedra around manganese. In agreement with the slight distortion of the MnO_6 octahedra in $LaMnO_3$ and $CaMnO_3$, the edges of these manganites exhibit a small prepeak and a single main peak at 16 eV and 20 eV respectively due to the $1s \rightarrow 4p_{x,y,z}$ transition. Conversely, for Mn_2O_3 and MnO_2, a wide spread of Mn-O distances induces a splitting of the three components of the $1s \rightarrow 4p_{x,y,z}$ transition as can be seen on the edges of these two oxides (Fig. 6a).

In Figures 6b and 6c are presented the Mn K-edges of the starting $Ln_{0.5}Ca_{0.5}MnO_3$ (Ln=La,Nd) and of the substituted compounds, $La_{0.5}Ca_{0.5}(Mn_{1-x}B_x)O_3$ (B=Cr, Co, Ni; $x = 0.08$) and $Ln_{0.5}Ca_{0.5}(Mn_{1-x}Cr_x)O_3$ (Ln=Nd;

Table 2. Formal charge, d_{Cr-O}, energy of main jump midheight and equivalent energies from edge integration at Cr K-edge for references and doped manganites compounds.

compounds	formal charge Cr	d_{Cr-O} in angström	energy of main jump midheight (eV) ± 0.3 eV	equivalent energies from edge integration (eV) ± 0.3 eV	references
Cr_2O_3	+3	Cr(1):3 × 1.95; 3 × 2.04	13.8	10.9	[35]
$NdCrO_3$	+3	Cr(1):4 × 1.975; 2 × 1.985	14.1	11.4	[36]
CrO_2	+4	Cr(1):4 × 1.78; 2 × 2.08	16.7	13.7	[37]
$K_2Cr_2O_7^{(*)}$	+6	Cr(1):1.54; 1.59; 1.69; 1.71 Cr(2):1.55; 1.57; 1.57; 1.86 Cr(3):1.59; 1.63; 1.68; 1.84 Cr(4):1.51; 1.61; 1.64; 1.75	17.8	11.0	[38]
$Sm_{0.5}Ca_{0.5}Cr_{0.05}Mn_{0.95}O_3$	+3		14.5	11.7	
$Sm_{0.5}Ca_{0.5}Cr_{0.10}Mn_{0.90}O_3$	+3		14.4	11.7	
$Nd_{0.5}Ca_{0.5}Cr_{0.05}Mn_{0.95}O_3$	+3		14.2	11.1	
$Nd_{0.5}Ca_{0.5}Cr_{0.10}Mn_{0.90}O_3$	+3		14.4	11.6	

$^{(*)}$: four tetrahedral sites

Sm; $x = 0.05$) together with two manganese references. In agreement with previous observations on the K-edges of manganites [26], the energy of the midheight of the main absorption jump can be correlated to the manganese formal charge even using a linear relationship. For instance, in this work, the midheight energies of the Mn K-edges of the $Ln_{0.5}Ca_{0.5}MnO_3$ (Ln=La, Nd) are the same, around 12.0 eV within 0.1 eV, whatever the rare earth (Tab. 3). From this result, a mean formal charge of 3.5 can be deduced for manganese as expected from the cation but also from the oxygen stoichiometries.

Now, considering the edges of the doped manganites, one can see a shift of the edges towards high energy by 0.3 to 0.5 eV whatever the nature of the dopant (Cr, Co, Ni). This energy shift is equivalent or higher than the reproducibility of the "Channel cut" monochromator position at the EXAFS1 station. It corresponds to an increase of the manganese formal charge in the substituted manganites with respect to the undoped manganites. Such an observation corroborates the results obtained for the formal charge of the dopant. In all cases, the substitution of manganese with an average oxidation state larger than three by species of lower formal charge (Ni^{2+}, Co^{2+} or Cr^{3+}) requires change compensation in order to keep the oxygen stoichiometry "O_3". Consequently an increase of the formal charge of manganese is induced by doping with those species.

Moreover, taking into account the charge balance in the chemical formula of the manganite, chromium owing to its higher formal charge (Cr^{3+}) compared to nickel and cobalt (Ni^{2+}, Co^{2+}), should induce a smaller average charge of manganese according to the XAS results if we admit that the "O_3" stoichiometry is maintained (Tab. 4). The manganese charge shifts allow edge energy shifts to be calculated with respect to the undoped manganites. The latter are compatible with the experimental ones (Tab. 4) although our experiments at Mn K-edge do not allow to discriminate $Mn^{3.54+}$ from $Mn^{3.63+}$.

4 Concluding remarks

The doping of the Mn sites in the charge-ordered manganites $Ln_{0.5}Ca_{0.5}MnO_3$ with Ni, Co or Cr, keep the dopants in their lower oxidation state (Ni^{2+}, Co^{2+} or Cr^{3+}). As a consequence, it induces an increase of the formal charge of manganese, so that the "O_3" stoichiometry of the perovskite is unchanged.

Such an increase of the formal charge of manganese is susceptible to destroy the charge ordering which exists in the undoped manganites $Ln_{0.5}Ca_{0.5}MnO_3$. Nevertheless, it can not alone explain the appearance of the metal-insulator transition which is unexpected in the Mn^{4+} rich perovskites, since $Ln_{0.5-x}Ca_{0.5+x}MnO_3$ manganites with $x \leq 0.10$ do not exhibit such properties.

Table 3. Formal charge, d_{Mn-O}, energy of main jump midheight and equivalent energies from edge integration at Mn-K-edge for references and doped manganites compounds.

compounds	formal charge Mn	d_{Mn-O} in angström	energy of main jump midheight (eV) ± 0.3 eV	equivalent energies from edge integration (eV) ± 0.3 eV	reference
Mn_2O_3	+3	Mn(1):2 × 1.96; 2 × 2.00; 2 × 2.04 Mn(2):1.53; 1.90; 1.99; 2.24 2.45; 2.56	12.9	10.4	[40]
$LaMnO_3$	+3	Mn(1):2 × 1.92; 2 × 1.97; 2 × 2.16	12.8	10.5	[41]
MnO_2	+4	Mn(1):2 × 1.90; 4 × 2.38	16.5	13.6	[42]
$CaMnO_3$	+4	Mn(1):2 × 1.89; 4 × 1.90	16.4	13.2	[43]
$La_{0.5}Ca_{0.5}MnO_3$	+3.5	Mn(1):2 × 1.925; 2 × 1.94; 2 × 1.96	14.6	12.1	
$La_{0.5}Ca_{0.5}Cr_{0.08}Mn_{0.92}O_3$	$+3.5+\delta$		14.8	12.3	
$La_{0.5}Ca_{0.5}Ni_{0.08}Mn_{0.92}O_3$	$+3.5+\delta$		15.1	12.4	
$La_{0.5}Ca_{0.5}Co_{0.08}Mn_{0.92}O_3$	$+3.5+\delta$		15.1	12.4	
$Nd_{0.5}Ca_{0.5}MnO_3$	+3.5	Mn(1):2 × 1.94; 2 × 1.945; 2 × 1.95	14.7	12.2	
$Nd_{0.5}Ca_{0.5}Cr_{0.05}Mn_{0.95}O_3$	$+3.5+\delta$		15.0	12.4	
$Sm_{0.5}Ca_{0.5}Cr_{0.05}Mn_{0.95}O_3$	$+3.5+\delta$		15.0	12.3	

Table 4. Substitution on Mn^{3+} site and on Mn^{4+} site after charge compensation.

compounds	formal charge of the Mn site	observed equivalent energies from edge integration (eV)	expected energy from formal charge of the Mn site (eV)
$LaMn^{3+}O_3$	+3	10.4	
$CaMn^{4+}O_3$	+4	13.6	
$La_{0.5}Ca_{0.5}Mn^{3+}_{0.5}Mn^{4+}_{0.5}O_3$	+3.5	12.1	12.0
$La_{0.5}Ca_{0.5}\{(Co^{2+}, Ni^{2+})_{0.08}Mn^{3+}_{0.34}Mn^{4+}_{0.58}\}O_3$	+3.63	12.4	12.4
$La_{0.5}Ca_{0.5}\{Cr^{3+}_{0.08}Mn^{3+}_{0.42}Mn^{4+}_{0.50}\}O_3$	+3.54	12.3	12.1
$Sm_{0.5}Ca_{0.5}\{Cr^{3+}_{0.05}Mn^{3+}_{0.45}Mn^{4+}_{0.50}\}O_3$	+3.525	12.3	12.1
$Nd_{0.5}Ca_{0.5}\{Cr^{3+}_{0.05}Mn^{3+}_{0.45}Mn^{4+}_{0.50}\}O_3$	+3.525	12.4	12.1

Thus, it is more likely that the doping elements participate directly themselves to the double exchange phenomena and/or to the Jahn-Teller distortion and modify deeply the crystal field of these manganites.

But, the understanding of such drastic changes in magnetic and transport properties of the manganites by transition metal doping will need a deeper investigation of the induced changes in the electronic structure and specially in the band structure. For instance, as shown recently [44], high resolution photoemission studies of the Fermi level should allow a direct investigation of the changes in the electronic levels involved in the upper valence band induced by transition metal doping.

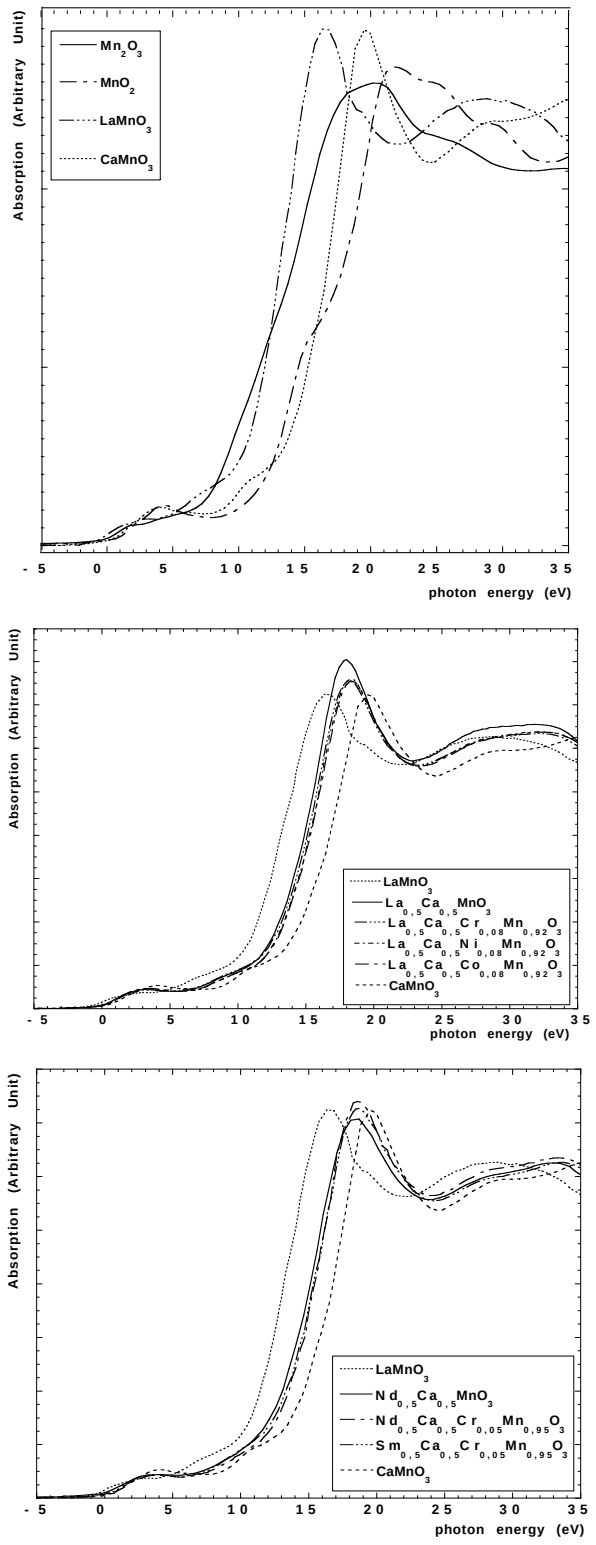

Fig. 6. (a) Normalized Mn K-edges at room temperature for manganese references. (b) Normalized Mn K-edges at room temperature for manganese references and $La_{0.5}Ca_{0.5}Mn_{0.92}B_{0.08}O_3$ (B=Cr; Ni; Co) – The edges of Ni and Co substituted compounds are superposed. (c) Normalized Mn K-edges at room temperature for manganese references and $Ln_{0.5}Ca_{0.5}Mn_{0.95}Cr_{0.05}O_3$ (Ln=Nd; Sm).

The authors are grateful to Dr Ph. Lacorre (University of Le Mans, France) and A. Barry (Trinity College Dublin, Ireland) for providing reference samples for the present study.

References

1. R.M. Kuster, J. Singleton, D.A. Keon, R.M. Greedy, W. Hayes, Physica B **155**, 362 (1989).
2. R. Von Hemmolt, J. Wecker, B. Holzapfel, L. Schultz, K. Samwer, Phys. Rev. Lett. **71**, 2331 (1993).
3. H.L. Ju, C. Kwon, Q. Li, R.L. Greene, T. Venkaten, Appl. Phys. Lett. **65**, 2108 (1994).
4. A. Maignan, Ch. Simon, V. Caignaert, B. Raveau, Solid State Commun. **96**, 623 (1995).
5. R. Mahesh, R. Mahendiran, A.K. Raychaudhury, C.N.R. Rao, J. Solid State Chem. **114**, 297 (1995).
6. S. Jin, H.M. O'Bryan, T.H. Tiefel, M. McCormack, W.W. Rhodes, Appl. Phys. Lett. **66**, 382 (1995).
7. A. Maignan, C. Martin, B. Raveau, Z. Phys. B, **102**, 19-24 (1997).
8. C. Martin, A. Maignan, B. Raveau, J. Mater Chem. **6**, 1245-1248 (1996).
9. C. Zener, Phys. Rev. **82**, 403 (1951).
10. P.W. Anderson, H. Hasegawa, Phys. Rev. **100**, 975 (1955).
11. P.G. De Gennes, Phys. Rev. **118**, 141 (1960).
12. A.J. Millis, P.B. Litlewood, B.I. Shraiman, Phys. Rev. Lett. **74**, 5144 (1995); A.J. Millis, B.I. Shraiman, R. Mueller, Phys. Rev. Lett. **77**, 175 (1996).
13. V. Caignaert, E. Suard, A. Maignan, Ch. Simon, B. Raveau, J. Magn. and Magn. Mater. **153**, L260 (1996); V. Caignaert, F. Millange, M. Hervieu, G. Mather, B. Raveau, E. Suard, P. Laffez, G. Van Tendeloo, Phys. Rev. B. (accepted).
14. J.L. Garcia-Munoz, M. Suaaidi, J. Fontcuberta, J. Rodriguez-Carvajal, Phys. Rev. B **55**, 34 (1997).
15. F. Studer, O. Toulemonde, V. Caignaert, P. Srivastava, J. Goedkoop, N. Brookes, in *Proceeding of 9th International Conference on X-Ray absorption fine structure*, J. Phys. IV France, **7**, (1997).
16. C. Meneghini, R. Cimino, S. Pascarelli, S. Mobilio, C. Raghu, D.D. Sarma, Phys. Rev. B **56**, 3520 (1997).
17. C.H. Booth, F. Bridges, G.H. Kwei, J.M. Lawrence, A.L. Cornelius, J.J. Neumeier, Phys. Rev. Lett. **80**, 853 (1998).
18. C.H. Booth, F. Briges, G.J. Snyder, T.H. Geeballe, Phys. Rev. B **54**, R15606 (1996).
19. B. Raveau, A. Maignan, C. Martin, J. Solid State Chem. **130**, 162 (1997).
20. A. Maignan, F. Damay, C. Martin, B. Raveau, Mater. Res. Bull. **32**, 965 (1997).
21. A. Barnabe, A. Maignan, M. Hervieu, F. Damay, C. Martin, B. Raveau, Appl. Phys. Lett. **71**, 3907 (1998).
22. A. Bianconi, *Synchrotron Radiation in Chemistry and Biology I*, edited by E. Mandelkow, Topics in Current Chemistry, Vol. 145 (Springer-Verlag, Berlin 1988).
23. R. Retoux, F. Studer, C. Michel, B. Raveau, A. Fontaine, E. Dartyge, Phys. Rev. B **41**, 1 (1990).
24. F. Studer, *High temperature superconductors*, edited by John J. Pouch, S.A. Alterowitz, R.R. Romanofsky, Trans. Tech. Publications, Aedemansdorff, Switzerland, Materials Science Forum 137-139 (1993), p. 187.
25. N. Merrien, F. Studer, C. Martin, A. Maignan, C. Michel, J. Sol. Stat. Chem. **101**, 237 (1992).

26. G. Subias, J. Garcia, M.G. Proietti, J. Blasco, Phys. Rev. B **56**, 8183 (1997).
27. M. Croft, D. Sills, M. Greenblatt, C. Lee, S.W. Cheong, K.V. Ramanujachary, D. Tran, Phys. Rev. B **55**, 8726 (1997).
28. G.H. Kwei, C.H. Booth, F. Bridges, M.A. Subramaniam, Phys. Rev. B **55**, R688 (1997).
29. F. Pertlik, Acta Cryst. C, **39** (1983).
30. G. Thornton, B.C. Tofield, A.W. Hewat, J. Solid State Chem. **61**, 301 (1986).
31. B. Grange, Z. Anorg. Allge. Chem. **433**, 152 (1977).
32. G. Demazeau, A. Marbeuf, M. Pouchard, P. Hagenmuller, J. Solid State Chem. **3**, 582 (1971).
33. N. Natoli, *Exafs and near edge structure*, edited by A. Bianconi, L. Incoccia, S. Stipcich, Springer Series in thermal physics 27, Frascati (Italy) September 13-17, (1983).
34. J.H. Park, S.W. Cheong, C.T. Chen, Phys. Rev. B **55**, 17, 11072 (1997).
35. P.D. Battle, T.C. Gibb, S. Nixon, W.T.A. Harrison, J. Solid State Chem. **75**, 21 (1988).
36. H. Taguchi, J. Solid State Chem. **118**, 367 (1995).
37. T.J. Swoboda, P. Arthur, N.L. Cox, J.N. Ingraham, A.L. Oppegard, M.S. Sadler, J. Appl. Phys. **32**, 374 (1961).
38. E.A. Kuz'min, V.V. Plyukhin, N.V. Belov, DANKA **173**, 1068 (1967).
39. K. Attenkofer, G. Schultz, in *Proceeding of 9th International Conference on X-Ray absorption fine structure*, J. Phys. IV France **7**, C4 (1997).
40. S. Geller, Acta Cryst. B **27**, 821 (1972).
41. R. Pauthenet, C. Veyret, J. Phys. France **31** (1970).
42. W.H. Bauer, Acta Crystall. B **24**, 1968 (1982).
43. K.R. Poeppelmeier, M.E. Leonowicz, J.C. Scanlon, J.M. Longo, W.B. Yelom, J. Solid State Chem. **45**, 71 (1982).
44. J.H. Park, E. Veskovo, H.J. Kim, C. Kwon, R. Ramesh, T. Venkatesen, Nature (1998) accepted.